

Porphyrinoids

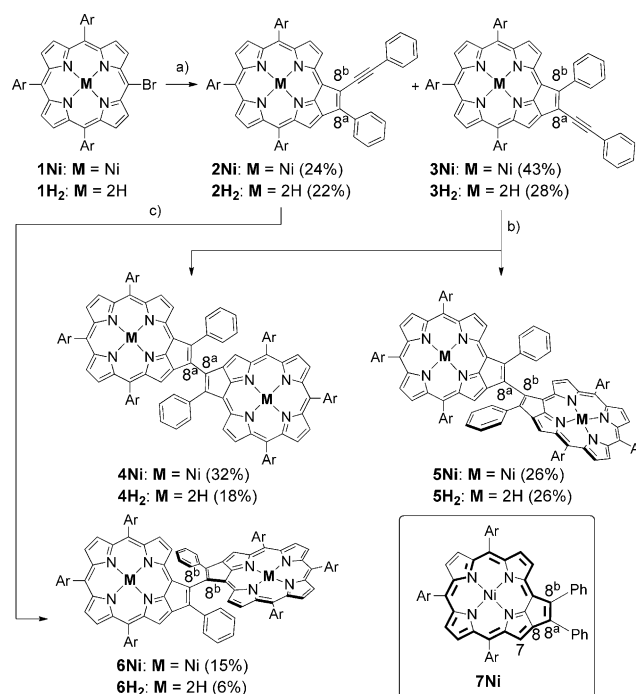
Synthesis of 7,8-Dehydropurpurin Dimers and Their Conversion into Conformationally Constrained β -to- β Vinylene-Bridged Porphyrin Dimers**

Norihito Fukui, Hideki Yorimitsu,* Jong Min Lim, Dongho Kim,* and Atsuhiko Osuka*

Abstract: 7,8-Dehydropurpurin has attracted much attention owing to the dual 18π - and 20π -electron circuits in its macrocyclic conjugation. The two-fold Pd-catalyzed [3+2] annulation of meso-bromoporphyrin with 1,4-diphenylbutadiyne furnished 7,8-dehydropurpurin dimers. The $8^a,8^b$ -linked dimer displays a red-shifted and enhanced absorption band in the NIR region and a small electrochemical HOMO–LUMO band gap as a consequence of efficient conjugation between the two coplanar 7,8-dehydropurpurin units. Treatment of this dimer with *N*-bromosuccinimide in chloroform and ethanol gave β -to- β vinylene-bridged porphyrin dimers. Owing to the highly constrained conformations, these dimers exhibit perturbed absorption spectra, small Stokes shifts, and high fluorescence quantum yields.

The 7,8-dehydropurpurins are intriguing porphyrinoids that exhibit altered absorption spectra, small HOMO–LUMO band gaps, and weakened aromaticity, as compared with standard porphyrins.^[1–4] These properties arise from the presence of dual 18π - and 20π -electron circuits that resonate in the conjugated macrocyclic network.^[1] Although a handful of 7,8-dehydropurpurin monomers have been synthesized in recent years, the chemistry of 7,8-dehydropurpurins remains relatively unexplored due to limited synthetic access to these macrocycles. In addition, there are no reports of multi-dehydropurpurinic compounds. Recently, we reported the efficient synthesis of 7,8-dehydropurpurin **7Ni** by Pd-catalyzed [3+2] annulation of meso-bromoporphyrin with diphe-

nylacetylene.^[2] Herein, we report the extension of this annulation reaction to the synthesis of directly linked 7,8-dehydropurpurin dimers **4M–6M** as the first examples of multi-dehydropurpurinic compounds (Scheme 1). Furthermore, dimers **4M** were efficiently converted into rigidly β -to- β vinylene-bridged porphyrins **8M** upon treatment with *N*-bromosuccinimide (NBS) in chloroform and ethanol. Zinc complexes **8Zn** exhibit fluorescence quantum yields of more than 0.17.



Scheme 1. Synthesis of **2M–6M** and the structure of $8^a,8^b$ -diphenyl-7,8-dehydropurpurin **7Ni**. Ar = 3,5-di-*tert*-butylphenyl. Reaction conditions: a) 1,4-diphenylbutadiyne (1.6 equiv for M = Ni, 1.5 equiv for M = 2H), (o-tol)₃P (28 mol %), [Pd₂(dba)₃] (7 mol %), NEt₃ (5 equiv), toluene, 110 °C; b) meso-bromoporphyrin (3.5 equiv for M = Ni, 3.4 equiv for M = 2H), (o-tol)₃P (2 equiv), [Pd₂(dba)₃] (50 mol %), NEt₃ (5 equiv), DMF, 110 °C; c) meso-bromoporphyrin (5 equiv), (o-tol)₃P (2 equiv), [Pd₂(dba)₃] (50 mol %), NEt₃ (5 equiv), DMF, 110 °C. dba = dibenzylideneacetone, DMF = *N,N*-dimethylformamide.

First, Pd-catalyzed [3+2] annulation^[2] of Ni^{II} meso-bromoporphyrin **1Ni** with 1,4-diphenylbutadiyne under slightly modified conditions^[5] gave alkynyl-7,8-dehydropurpurins **2Ni** and **3Ni** (Scheme 1a,b). Atmospheric pressure chemical ionization (APCI) mass spectra of **2Ni** and **3Ni** display parent ion peaks at 1130.5693 and 1130.5711, respec-

[*] N. Fukui, Prof. Dr. H. Yorimitsu, Prof. Dr. A. Osuka
Department of Chemistry, Graduate School of Science
Kyoto University, Sakyo-ku, Kyoto 606-8502 (Japan)
E-mail: yori@kuchem.kyoto-u.ac.jp
osuka@kuchem.kyoto-u.ac.jp

Prof. Dr. H. Yorimitsu
ACT-C (Japan) Science and Technology Agency (Japan)
Dr. J. M. Lim, Prof. Dr. D. Kim
Spectroscopy Laboratory for Functional π -Electronic Systems and
Department of Chemistry, Yonsei University, Seoul 120-749 (Korea)
E-mail: dongho@yonsei.ac.kr

[**] The work at Kyoto was supported by Grants-in-Aid from MEXT (24106721 “Reaction Integration” and 25107002 “Science of Atomic Layers”) and from JSPS (25220802 Scientific Research (S), 24685007 Young Scientists (A), and 23655037 Exploratory Research). The work at Yonsei was supported by the Midcareer Researcher Program (2010-0029668) of the Ministry of Education, Science, and Technology (MEST) of Korea. The work was supported by Global Research Laboratory (GRL) Program (2013-8-1472) of the Ministry of Education, Science, and Technology (MEST) of Korea.

Supporting information for this article is available on the WWW under <http://dx.doi.org/10.1002/anie.201400632>.

tively (calc'd for $C_{78}H_{80}N_4Ni$, m/z 1130.5731 $[M]^+$). The structures of **2Ni** and **3Ni** have been unequivocally determined by X-ray diffraction analysis (Figure 1). The $C8^a-C8^b$ bond lengths are 1.406 Å in **2Ni** and 1.405 Å in **3Ni**, which is strong evidence for sp^2 hybridization. The 1H NMR spectra of **2Ni** and **3Ni** in $CDCl_3$ (see the Supporting Information) exhibit considerably decreased diatropic ring currents, as reported in the other 7,8-dehydropurpurins.^[1–4]

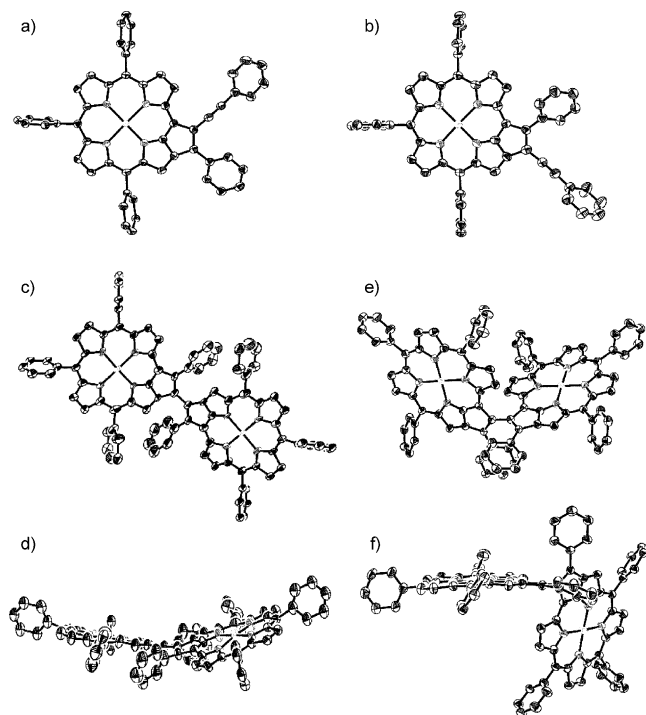


Figure 1. X-Ray crystal structures. a) Top view of **2Ni**, b) top view of **3Ni**, c) top view and d) side view of **4Ni**, e) front view and f) side view of **6Ni**. Thermal ellipsoids are drawn at the 50% probability level for **2Ni**, and at the 30% probability level for **3Ni**, **4Ni**, and **6Ni**. Solvent molecules, *tert*-butyl groups and all hydrogen atoms are omitted for clarity.

In the next step, the [3+2] annulation reaction of **1Ni** with **3Ni** was attempted under similar conditions. The reaction was sluggish in toluene but proceeded smoothly in $DMF^{[6]}$ to provide 7,8-dehydropurpurin dimers **4Ni** and **5Ni** in 32% and 26% yields, respectively. The structure of **4Ni** has been determined by X-ray analysis (Figure 1 c,d), in which the two 7,8-dehydropurpurin units were linked at the $C8^a$ and $C8^{a'}$ positions with a $C8^a-C8^{a'}$ bond distance of 1.451 Å, and are arranged in a coplanar manner with a small dihedral angle of 35.55°. The minor dimer, which has a $C8^a-C8^{b'}$ connection, has thus been assigned as **5Ni**. Dimers **4Ni** and **5Ni** were isolated as purple and brown solids, respectively. These results have demonstrated that a peripherally alkylnated 7,8-dehydropurpurin such as **3Ni** can serve as an alkyne substrate in the Pd-catalyzed [3+2] annulation reaction. Encouraged by the successful formation of **5Ni**, which should be formed by a more-congested carbopalladation step, the [3+2] annulation reaction of **1Ni** with **2Ni** has been also attempted under similar conditions, and furnished **6Ni** in 15% yield as brown

solids with a 42% recovery of **2Ni** (Scheme 1). The dimer **6Ni** was expected to be much more sterically congested. This has been confirmed by its crystal structure, as shown in Figure 1 e,f. In **6Ni**, the two 7,8-dehydropurpurin units are linked together with a larger dihedral angle of 74.55° and a longer $C8^b-C8^{b'}$ bond distance of 1.462 Å. Free base 7,8-dehydropurpurins **2H₂** and **3H₂** and dimers **4H₂**, **5H₂**, and **6H₂** were similarly synthesized.

The UV/Vis/NIR absorption spectra of **3Ni–6Ni** in CH_2Cl_2 are shown in Figure 2. The absorption spectra of **2Ni** and **3Ni** are similar, showing split Soret bands located at

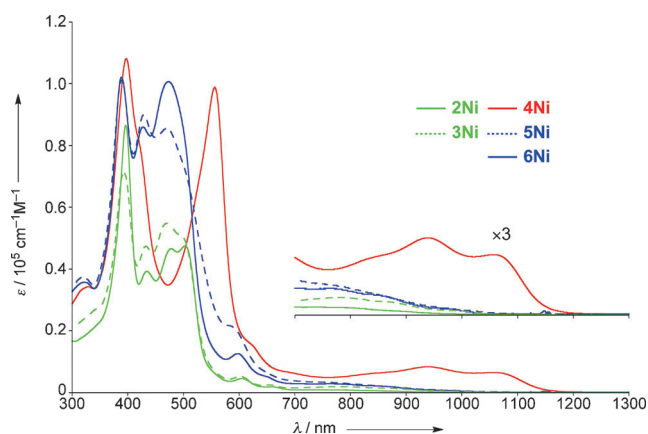


Figure 2. UV/Vis/NIR absorption spectra of **2Ni–6Ni** in CH_2Cl_2 .

350–550 nm, almost featureless Q-like bands around 600 nm, and weak and extremely broad bands reaching out to around 1050 nm. The broad and weak bands reflect forbidden HOMO–LUMO transitions related to a 20π -antiaromatic 7,8-dehydropurpurin system, as previously observed.^[1–4] The absorption spectra of **5Ni** and **6Ni** are both roughly similar to those of **2Ni** and **3Ni**, except for some intensification of the longer split Soret bands. In contrast, the absorption spectrum of **4Ni** is more distinguished from those of **5Ni** and **6Ni**, showing split Soret bands at 397 and 556 nm, and well-defined near-infrared (NIR) bands at 939 and 1056 nm. These characteristic spectral features have been interpreted in terms of effective conjugation of the two 7,8-dehydropurpurin units in **4Ni**, which is aided by its coplanar structure. On the other hand, the electronic conjugation is interrupted in **5Ni** and **6Ni**, owing to the tilted relationship between their subunits.

The electrochemical properties of **2Ni–7Ni** were studied by cyclic voltammetry (CV) in CH_2Cl_2 (Table 1). Reference monomer **7Ni** exhibited two reversible oxidation and reduction waves. Monomers **2Ni** and **3Ni** exhibited similar waves, but their second oxidation waves became irreversible and their reduction waves were shifted to lower potentials versus those of **7Ni**. These CV data allowed for the estimation of electrochemical HOMO–LUMO band gap: 1.53 and 1.56 eV for **2Ni** and **3Ni**, respectively. Dimer **4Ni** showed oxidation waves at –0.05, 0.17, and 0.88 V, and reduction waves at –1.31 and –1.48 V. The two lower oxidation waves have been interpreted as split first potentials with $\Delta E = 0.22$ V, owing to

Table 1: Redox potentials of **2Ni–7Ni**.^[a]

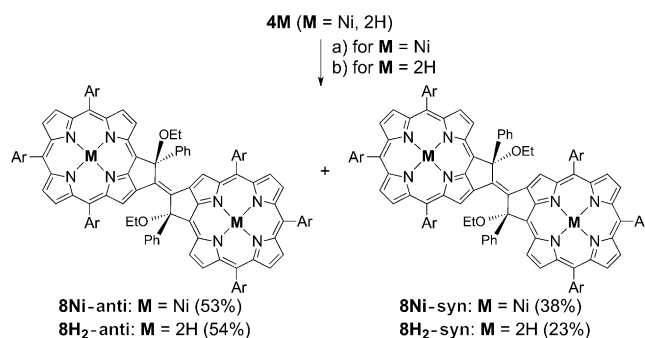
	Oxidation [V]				Reduction [V]		$E^{1/2}_{ox1} - E^{1/2}_{red1}$ [eV]
	$E^{1/2}_{ox1}$	$E^{1/2}_{ox2}$	$E^{1/2}_{ox3}$	$E^{1/2}_{ox4}$	$E^{1/2}_{red1}$	$E^{1/2}_{red2}$	
2Ni	0.22	–	–	–	–1.31	–1.77	1.53
3Ni	0.17	–	–	–	–1.39	–1.76	1.56
4Ni	–0.05	0.17	0.88	–	–1.31	–1.48	1.26
5Ni	0.08	0.29	0.73	–	–1.44	–1.57	1.52
6Ni	0.17	0.35	0.58	0.73	–1.45	–1.56	1.62
7Ni	0.19	0.64	–	–	–1.47	–1.90	1.63

[a] The redox potentials were measured by cyclic voltammetry in anhydrous CH_2Cl_2 , with Bu_4NPF_6 (0.1 M) as a supporting electrolyte and Ag/AgClO_4 as a reference electrode; ferrocene/ferrocenium ion couple was used as an external reference.

the electronic interaction of the two 7,8-dehydropurpurins. The electrochemical HOMO–LUMO gap has been calculated to be 1.26 eV, which is distinctly smaller than those of dimers **5Ni** (1.52 eV) and **6Ni** (1.62 eV).

Time-dependent density functional theory (TD-DFT) calculations (Gaussian) at the B3LYP/6-31G*(C,H,N) + LANL2DZ(Ni) level have been performed on dimers **4Ni** and **6Ni** along with **7Ni** (Supporting Information, Figures S60–65).^[7] Unlike Ni^{II} -porphyrin, **7Ni** has non-degenerate HOMO-1, HOMO, LUMO, and LUMO+1 that lie at distinctly different energy levels. The HOMO–LUMO excitation of **7Ni** is symmetry forbidden, for which the oscillator strength was calculated to be ca. 0.0244. In dimer **6Ni**, the interaction of two HOMOs (LUMOs) of 7,8-dehydropurpurin units led to a slightly perturbed HOMO and HOMO-1 (LUMO and LUMO+1). The energy differences are quite small: 0.145 eV for the HOMO–HOMO-1 energy gap and 0.085 eV for the LUMO–LUMO+1 energy gap. In contrast, larger energy differences are calculated for **4Ni**: 0.522 eV for the HOMO–HOMO-1 energy gap and 0.367 eV for the LUMO–LUMO+1 energy gap. More importantly, the HOMO–LUMO transition in **4Ni** becomes symmetry-allowed and its oscillator strength was calculated to be 0.2399, which is consistent with the observed moderate absorbance of the NIR bands. The HOMO–LUMO transition in **6Ni** remains symmetry prohibited and the oscillator strength was calculated to be 0.0163. The HOMO–LUMO gaps of **4Ni** and **6Ni** were calculated to be 1.684 and 2.002 eV, respectively, showing the same trend with the experimental results.

The two fused five-membered rings in **4Ni** are well conjugated and were expected to show high reactivity. This was indeed the case, and **4Ni** cleanly reacted with *N*-bromosuccinimide in CHCl_3 and ethanol. To our surprise, no brominated products were obtained. Instead, we were delighted to isolate β -to- β vinylene-bridged porphyrin dimer **8Ni-anti** and **8Ni-syn** (Scheme 2). They would be formed through bromoetherification of the butadiene linkage followed by nucleophilic substitution of the resulting highly reactive bromide with ethanol. X-ray crystallographic analysis unambiguously revealed the interesting structure of **8Ni-anti** (Figure 3), in which the two Ni^{II} porphyrin units are bridged in a coplanar manner by a vinylene unit that is fixed by two sp^3 carbons (Figure 4). Although a similar conforma-



Scheme 2. Structures and synthesis of **8**. Ar = 3,5-di-*tert*-butylphenyl. Reaction conditions: a) NBS (1.0 equiv), pyridine (2 drops), $\text{CHCl}_3/\text{EtOH}$, 0°C; b) NBS (1.0 equiv), pyridine (2 drops), $\text{CHCl}_3/\text{EtOH}$, 0°C; then $\text{Zn}(\text{OAc})_2 \cdot 2\text{H}_2\text{O}$, $\text{CH}_2\text{Cl}_2/\text{MeOH}$.

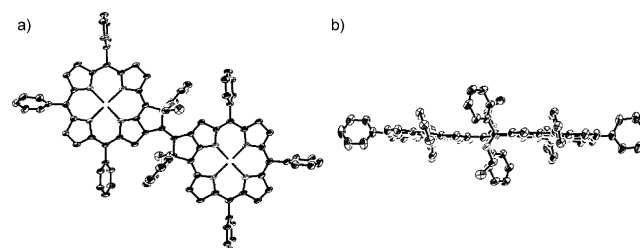


Figure 3. X-Ray crystal structures. a) Top view and b) side view of **8Ni-anti**. Thermal ellipsoids are drawn at the 50% probability level. Solvent molecules, *tert*-butyl groups, and all hydrogen atoms are omitted for clarity.

tionally fixed vinylene-bridged dimer was reported for pheophorbides,^[8] this is, to the best of our knowledge, the first example of porphyrin congeners.^[9] Through similar treatment, Zn^{II} -complexes **8Zn-anti** and **8Zn-syn** were prepared from **4H2** followed by zinc metalation (Scheme 2). The UV/Vis absorption and fluorescence spectra of **8Zn-anti** and **8Zn-syn** are shown in Figure 4. These two isomers show largely perturbed absorption spectra that are panchromatic up to ca. 650 nm. Characteristically, the Q bands at 637 nm are sharp and intensified, reflecting the enhanced transition

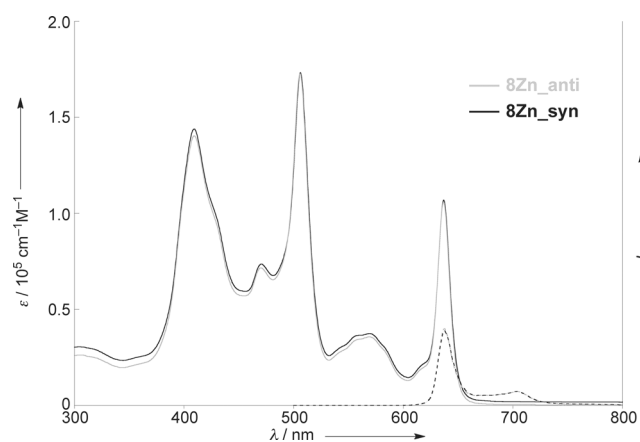


Figure 4. UV/Vis absorption (solid lines) and fluorescence (dashed lines) spectra of **8Zn-anti** and **8Zn-syn** in CH_2Cl_2 .

dipole moment along the long molecular axis. The rigidly held conjugated structures of **8Zn** result in very small Stokes shifts (15 cm^{-1}). In addition, **8Zn-anti** and **8Zn-syn** exhibit high fluorescence quantum yields, 0.172 and 0.173, respectively, and fluorescence lifetimes of 1.73 ns. Based on these data, the radiative rate constants of **8Zn-anti** and **8Zn-syn** have been estimated to be $9.9 \times 10^7\text{ s}^{-1}$, which are distinctly larger than that of Zn^{II} tetraphenylporphyrin ($1.5 \times 10^7\text{ s}^{-1}$).^[10,11] The larger radiative rates of **8Zn** can be ascribed to the large transition dipole moments along the long molecular axis.

In summary, two-fold Pd-catalyzed [3+2] annulation of *meso*-bromoporphyrin **1M** with 1,4-diphenylbutadiyne furnished 7,8-dehydropurpurin dimers **4M**, **5M**, and **6M** through **2M** or **3M**. Whereas the electronic interactions between the 7,8-dehydropurpurins are weak in **5M** and **6M**, the two 7,8-dehydropurpurin units are effectively conjugated in **4M**, as indicated by the red-shifted and enhanced absorption bands in the long wavelength region, the small electrochemical HOMO–LUMO band gap, and TD-DFT calculations. The dimer **4M** was converted into β -to- β vinylene-bridged porphyrin dimers **8M**, which display largely perturbed absorption spectra with small Stokes shifts and high fluorescence quantum yields, reflecting the well-conjugated electronic networks and constrained conformations. These attractive attributes are promising for use in many elaborate applications. Further studies related to this work are actively in progress in our laboratories.

Received: January 21, 2014
Published online: March 18, 2014

Keywords: 7,8-dehydropurpurin · conjugation · dimerization · porphyrinoids

- [1] For thiophene-fused 7,8-dehydropurpurins, see: Y. Mitsushige, S. Yamaguchi, B. S. Lee, Y. M. Sung, S. Kuhri, C. A. Schierl, D. M. Guldi, D. Kim, Y. Matsuo, *J. Am. Chem. Soc.* **2012**, *134*, 16540.
[2] A. K. Sahoo, S. Mori, H. Shinokubo, A. Osuka, *Angew. Chem.* **2006**, *118*, 8140; *Angew. Chem. Int. Ed.* **2006**, *45*, 7972.

- [3] A. Nakano, N. Aratani, H. Furuta, A. Osuka, *Chem. Commun.* **2001**, 1920.
[4] For benzo-fused 7,8-dehydropurpurins, see: a) S. Fox, R. W. Boyle, *Chem. Commun.* **2004**, 1322; b) D.-M. Shen, C. Liu, Q.-Y. Chen, *Chem. Commun.* **2005**, 4982; c) D.-M. Shen, C. Liu, Q.-Y. Chen, *J. Org. Chem.* **2006**, *71*, 6508; d) S. Hayashi, Y. Matsubara, S. Eu, H. Hayashi, T. Umeiyama, Y. Matano, H. Imahori, *Chem. Lett.* **2008**, *37*, 846; e) G. Bringmann, D. C. G. Götz, T. A. M. Gulder, T. H. Gehrke, T. Bruhn, T. Kupfer, K. Radacki, H. Braunschweig, A. Heckmann, C. Lambert, *J. Am. Chem. Soc.* **2008**, *130*, 17812; f) T. D. Lash, B. E. Smith, M. J. Melquist, B. A. Godfrey, *J. Org. Chem.* **2011**, *76*, 5335; g) A. M. V. M. Pereira, M. G. P. M. S. Neves, J. A. S. Cavaleiro, C. Jeandon, J.-P. Gisselbrecht, S. Choua, R. Ruppert, *Org. Lett.* **2011**, *13*, 4742; h) T. Ishizuka, Y. Saegusa, Y. Shiota, K. Ohtake, K. Yoshizawa, T. Kojima, *Chem. Commun.* **2013**, *49*, 5939; i) N. Fukui, W.-Y. Cha, S. Lee, S. Tokuji, D. Kim, H. Yorimitsu, A. Osuka, *Angew. Chem.* **2013**, *125*, 9910; *Angew. Chem. Int. Ed.* **2013**, *52*, 9728.
[5] Although we used NCy_2Me (Cy = cyclohexyl) as the base in the previously reported procedures, use of NEt_3 enhanced the yield of **2Ni** and **3Ni**.
[6] a) R. C. Larock, E. K. Yum, *J. Am. Chem. Soc.* **1991**, *113*, 6689; b) G. Zeni, R. C. Larock, *Chem. Rev.* **2006**, *106*, 4644.
[7] Gaussian09, revision A.02, M. J. Frisch, et al. Gaussian, Inc.: Wallingford, CT, **2009**.
[8] L. Jaquinod, M. O. Senge, R. K. Pandey, T. P. Forsyth, K. M. Smith, *Angew. Chem.* **1996**, *108*, 1982; *Angew. Chem. Int. Ed. Engl.* **1996**, *35*, 1840.
[9] For β -to- β vinylene-bridged porphyrin dimers, see: a) Z. I. Zhilina, Y. V. Ishkov, I. S. Voloshanovskii, A. S. A. Andronati, D. L. Officer, *Tetrahedron Lett.* **1993**, *34*, 8531; c) E. G. Levinson, N. A. Reztsova, A. F. Mironov, *Mendeleev Commun.* **1995**, *5*, 44; d) A. K. Burrell, D. L. Officer, *Synlett* **1998**, 1297; e) S. Hiroto, K. Suzuki, H. Kamiya, H. Shinokubo, *Chem. Commun.* **2011**, 47, 7149; f) X. Jiang, P. Li, Y. Wang, Q. Shen, J. Tao, W. Shi, *Chin. J. Chem.* **2012**, *30*, 405.
[10] The fluorescence quantum yield and lifetime of Zn^{II} tetraphenylporphyrin were reported to be 0.033 and 2.2 ns; see: J.-P. Strachan, S. Gentemann, J. Seth, W. A. Kalsbeck, J. S. Lindsey, D. Holten, D. F. Bocian, *J. Am. Chem. Soc.* **1997**, *119*, 11191.
[11] The quantum yield of Zn^{II} triphenylporphyrin was measured to be 0.023 by our apparatus.